Optik 145 (2017) 398–406

Contents lists available at ScienceDirect

Optik

journal homepage: www.elsevier.de/ijleo

Original research article

Design and characterization of a low-loss, dispersion-flattened photonic crystal fiber for terahertz wave propagation

Md. Saiful Islam[a,*], Jakeya Sultana[b], Javid Atai[c], Mohammad Rakibul Islam[b], Derek Abbott[a]

[a] School of Electrical and Electronic Engineering, University of Adelaide, SA 5005, Australia
[b] Department of Electrical and Electronic Engineering, Islamic University of Technology, Gazipur, 1704, Bangladesh
[c] School of Electrical & Information Engineering, The University of Sydney, NSW 2006, Australia

ARTICLE INFO

Article history:
Received 1 April 2017
Received in revised form 23 July 2017
Accepted 29 July 2017

Keywords:
Terahertz
Photonic crystal fibers
Dispersion
Micro-structured fibers
Effective material loss

ABSTRACT

A porous core photonic crystal fiber, based on Topas, with ultra-low effective material loss and near zero flattened dispersion properties is proposed for efficient polarization preserving transmission of terahertz waves. The Finite Element Method (FEM) with a Perfectly Matched Layer (PML) boundary condition is used to compute the modal characteristics of the fiber that confirms a lower Effective Material Loss (EML) of 0.034 cm^{-1}, lower confinement loss of the order of $10^{-3.7}$ cm^{-1}, higher effective mode area of 0.6×10^6 μm^2 and a flattened dispersion variation of 0.09 ps/THz/cm. In addition, some other characteristics including birefringence, single mode operation, core power fraction and Figure of Merit (FOM) of the proposed fiber are also discussed. To simplify the fabrication process, only circular shaped air holes with a conventional hexagonal structure in the cladding is deployed. It is anticipated that, this newly proposed waveguide will open a new window for further terahertz research and broadband transmission of terahertz radiation.

1. Introduction

The 0.1–10 THz frequency range is loosely defined as the terahertz frequency band [1,2]. It lies in the transition region between optical and electrical frequencies making it both challenging and an area of frontier science that motivates further research. The terahertz band has gained significant interest due to its multidisciplinary applications including medical imaging [3,4], bio-sensing, security screening [5,6], spectroscopy [7], hybridization of DNA [8] and communication [9]. To widen its areas of application, reliable and efficient waveguides are of significant interest.

In recent years, researchers have proposed several waveguides [10–14] for transmitting terahertz signals efficiently. It is observed that, most of the proposed waveguides have high material absorption loss, and this has led to a preference for terahertz transmission in free space. Transmission of terahertz waves using free space causes a number of undesirable issues, including path loss, uncertain absorption loss, and difficult alignment.To overcome these problems, porous core photonic crystal fibers have recently been proposed for the terahertz regime. The key design parameters of porous core photonic crystal fibers are core diameter, frequency, air hole size, arrangement of air holes and distance, which can be freely designed based

* Corresponding author.
E-mail address: mdsaiful.islam@adelaide.edu.au (Md.S. Islam).

http://dx.doi.org/10.1016/j.ijleo.2017.07.061
0030-4026/

on the requirements of spcific applications. There are several bulk materials that can be used to design terahertz waveguides. These include polymethyl–methacrylate (PMMA) [15], Teflon [14], high density polyethylene (HDPE) [16], Topas [17] and Zeonex [18]. Topas is chosen as the base material of our proposed fiber because of its unique desirable characteristics that include, (i) lower material absorption loss of about 0.2 cm^{-1} at 1 THz frequency [22], (ii) higher glass transition temperature T_g than PMMA [19], (iii) multi-antibody bio-sensing [20], (iv) humidity insensitive [21], (v) excellent biocompatibility, (vii) constant refractive index $n = 1.53$ in the frequency range of 0.1–1.5 THz [22], (viii) negligibly hygroscopic [23], and it does not absorb water vapor, which is advantageous for manufacturing terahertz waveguides. In addition, Topas can be used in combination with Zeonex to make step index fibers [24]. In recent years, researchers have proposed several [25–32,38] Topas based PCFs for terahertz wave transmission. In 2012, Bao et al. [25] proposed a honeycomb terahertz fiber that shows an effective material loss of 1.5 cm^{-1} at 1.0 THz. The loss is high and the fabrication of the honeycomb fiber is difficult. In the same year, Uthman et al. [39] proposed a porous core low loss photonic crystal fiber. Using Teflon as the base material they claimed that using porous core and porous cladding the core power fraction can be increased significantly that consequently reduce the effect of material loss. In 2013, Liang et al. [26] proposed a porous core photonic band gap fiber which shows an EML of 0.432 cm^{-1} and dispersion variation of less than 2.5 ps/THz/cm. Later, Kaijage et al. [27] proposed an octagonal structure of photonic crystal fiber for terahertz wave guidance. They demonstrated an EML of 0.070 cm^{-1} at 1 THz frequency. However, they did not mention the dispersion properties of the fiber. In 2015, Islam et al. [28] proposed a rotated hexagonal porous core single mode fiber that shows an EML of 0.066 cm^{-1} and a core power fraction of 40%. Furthermore, Hasanuzzaman et al. [41], proposed a novel photonic crystal fiber incorporating kagome lattice and hexagonal core. They were able to provide an EML of 0.034 cm^{-1}, negligible confinement loss at 1 THz frequency. They also obtained a near zero flattened dispersion variation of 0.60565 ± 0.13955 ps/THz/cm within the frequency range of 0.75–1.15 THz. However, the fabrication of kagome-structured fiber is more challenging than that of fibers with only circular shaped air holes. For further improvement, in 2016, Saiful et al. [29] proposed a circular photonic crystal fiber and were able to reduce the EML to 0.053 cm^{-1} with a dispersion variation of 0.25 ps/THz/cm. A square lattice porous core photonic crystal fiber with an EML of 0.076 cm^{-1} and confinement loss of the order of 10^{-3} cm^{-1} was also proposed in Ref. [30]. Later, for terahertz wave guidance, a Teflon based polarization maintaining PCF has been proposed by Aming et al. [40]. They claimed that more than 85% of the total power can be confined in the air hole region that causes the reduction of modal loss to 85%. In addition, implementation of unequal sized air holes in the core region increases the birefringence. In 2016, Hasan et al. [31] proposed a bend insensitive porous fiber, where they were able to show an EML of 0.089 cm^{-1} and higher dispersion variation of 1.04 ± 0.27 ps/THz/cm without investigating the single mode properties of their proposed fiber. Then, an octagonal lattice with a rotated hexagonal core structure was proposed in Ref. [32], where it is shown that, the material absorption loss is reduced to 0.047 cm^{-1} with dispersion flatness of 0.15 ps/THz/cm. Recently, in 2017, more advanced work was proposed in Ref. [38], where the authors were able to reduce the EML further to 0.043 cm^{-1} with near zero dispersion flattened properties. The above works suggest there is great scope for PCF improvement in consideration of EML, confinement loss, bending loss, core power fraction, birefringence, dispersion, modal effective area and other relevant properties.

In this paper, a Topas based hybrid photonic crystal fiber containing the combination of rectangular and triangular structure in the core surrounding by an asymmetric rotated hexagonal structure in the cladding is proposed. At optimal design parameters, our design goals are to achieve as low material absorption loss as possible, negligible confinement loss, higher core power fraction, higher birefringence, higher effective mode area and ultra-flattened dispersion. To make the fabrication possibilities easier, only circular shaped air holes are used in both core and cladding of the proposed fiber.

2. Design methodology

The schematic diagram of the proposed hybrid porous core PCF is shown in Fig. 1. The commercially available full-vector finite element method based software COMSOL v 4.2 is used to compute the modal characteristics of the fiber. Five rings of an asymmetric hexagonal structure are used in the cladding while the core is a combination of rectangular and triangular structure. It is demonstrated that by introducing such structure inside the asymmetric-hexagonal cladding reduces the effective material loss (EML) and higher air filling fraction (AFF) makes the dispersion properties flat. The complete mesh of the proposed waveguide consists of 524 vertex element, 18272 boundary elements and 234467 total elements.

All the air holes in the cladding region are of same size with radius r_1. In the cladding, the spacing between air holes of two adjacent rings and that of the same rings is related by $\Lambda_1 = 0.765\Lambda$. For the core, the spacing between air holes is defined as Λ_c. Through the whole numerical analysis, the air filling fraction (AFF) d/Λ of the cladding was kept fixed at 0.85 for an optimal confinement factor because further increase overlaps the air holes, causing fabrication difficulties. In the meantime, at the core, the AFF is varied intentionally which mostly determined by the core porosity. Porosity is defined as the ratio of air hole area to the total cross-section area of the core. A perfectly matched layer boundary condition has been used at the outer part of the cladding, which is about 10% of the fiber radius.

It is important to consider the practical implementation of the fiber. There are several ways to fabricate PCF. The most commonly used methods are capillary stacking, drilling, stack and draw, extrusion and sol-gel etc. The Max Plank Institute fabricated several PCFs for a different lattice structure [33]. Almost all types of structure can be fabricated by the extrusion technique proposed by Kiang et al. [34]. As our proposed fiber consists of only circular shaped air holes and higher porosity, capillary stacking [31] and sol-gel [35] techniques are best suited as they both can be used to fabricate circular shaped air holes.

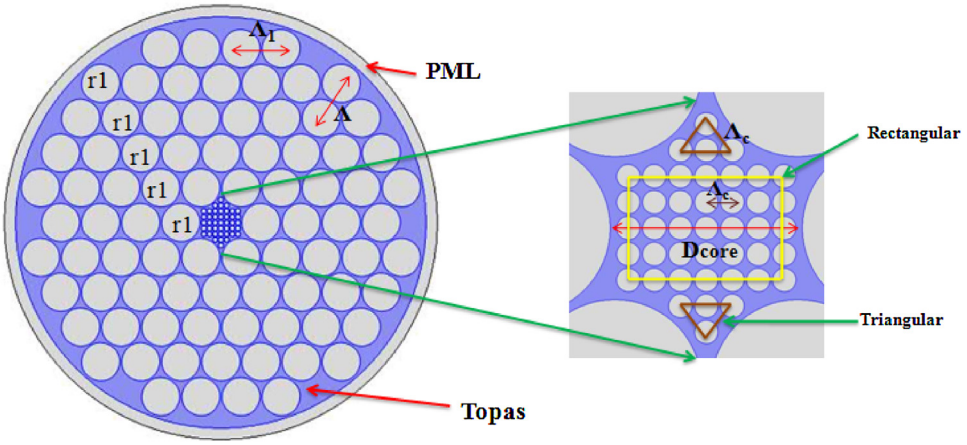

Fig. 1. Cross section of the proposed hybrid porous core fiber.

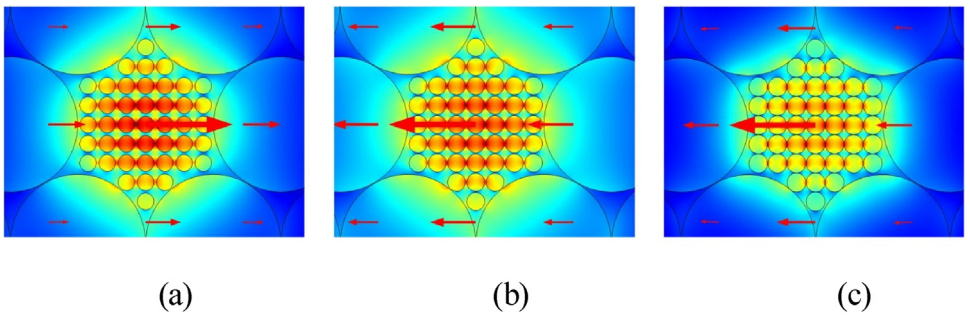

Fig. 2. Mode field distribution of the proposed PCF for (a) 64% (b) 74% (c) 84% porosity.

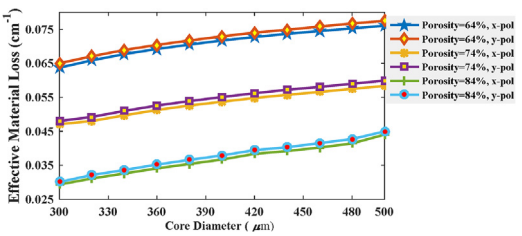

Fig. 3. EML vs Core diameter at $f = 1$ THz for orthogonal polarization mode.

3. Simulation & result

For different porosity values (64%, 74% and 84%), the fundamental mode field profile is shown in Fig. 2. It is observed that, mode fields are confined to the core, which is essential for efficient terahertz propagation. It is also observed from the same figure that, with the increase of core porosity, the index change between core and cladding is reduced and thus mode fields spread towards the cladding.

In terahertz frequency bands, most polymer materials are highly absorbent and it is a significant challenge in designing an efficient terahertz waveguide. The so-called material absorption loss or effective material loss can be calculated by [32],

$$\alpha_{\text{eff}} = \sqrt{\frac{\varepsilon_0}{\mu_0}} \left(\frac{\int_{\text{mat}} n_{\text{mat}} |E|^2 \alpha_{\text{mat}} dA}{|\int_{\text{all}} S_z dA|} \right) \tag{1}$$

where, ε_0 and μ_0 indicates the relative permittivity and permeability in vacuum respectively, α_{mat} is the bulk material absorption loss of Topas, n_{mat} indicates the refractive index of the background material and S_z is the z-component of the Poynting vector . Where, E and H are the electric and magnetic field components, respectively. Here, the integration of the numerator of Eq. (1) is carried out over the solid material region whereas the integration of the denominator is carried out over the whole region. It is observable from Fig. 3 that, as the core diameter increases the amount of solid material inside the

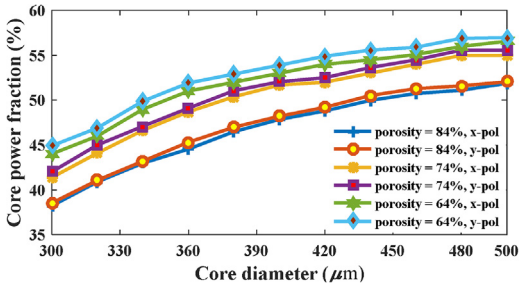

Fig. 4. Core power fraction vs core diameter at $f = 1$ THz for orthogonal polarization modes.

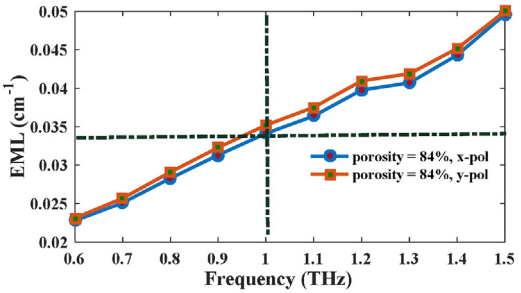

Fig. 5. EML vs frequency at optimal design parameters for orthogonal polarization modes.

core also increases that inturn increases the value of EML. It is also observed from Fig. 3 that, as the porosity increases the amount of solid material inside the core decreases, which consequently scaled down the EML. It is observed that, a minimal amount of EML is obtained at 300 μm but we choose 360 μm as optimal because at 300 μm the core power fraction is very low and confinement loss is very high.

The amount of modal power transferring through different regions of a PCF is known as mode power fraction. The mode power fraction can be calculated by [32],

$$\eta' = \frac{\int_X S_z dA}{\int_{all} S_z dA}, \tag{2}$$

where, the integration of the numerator is carried out over the region of interests and the integration of the denominator is done over the total area of the fiber. Fig. 4 describes the behavior of core power fraction with respect to core diameter at different porosity values. It is observed that, as the core diameter increases, the core power fraction also increases. We have seen that, core power fraction is maximum at 64% core porosity but we cannot choose that as optimal hence the value of EML at 64% porosity is higher than the other mentioned porosity values. We can also see that, the core power fraction values are higher at 500 μm, here we cannot also choose that point as optimum because EML is higher at that point. Upon observing Fig. 3 and 4, It can be observed that 360 μm core diameter and 84% core porosity can be considered as optimal design parameters, as at that point the obtained EML is as low as 0.034 cm^{-1} and core power fraction of 44%, which seems to be sufficient for efficient terahertz wave transmission.

At 360 μm core diameter and 84% porosity, Fig. 5 shows the characteristics of EML with respect to frequency. Here, it is observed that the EML is not constant but increases linearly with frequency [25]. This is because, the material absorption loss is proportional to frequency hence increasing frequency also increases the EML. So, according to the empirical formula [25]: $\alpha(\nu) = \nu^2 + 0.63\nu - 0.13$ [dB/cm], it is experimentally demonstrated that, the bulk material absorption loss depends on frequency.

This matter is carefully handled when calculating the frequency response of EML of our proposed PCF. It is seen that, EML is lower at 0.6 THz but we cannot choose that as optimal hence core power fraction is low at that point. Again, from Fig. 6 it can be seen that, at 0.6 THz the obtained confinement loss is higher than higher frequencies. Hence, we choose 1 THz as optimum where obtained EML is 0.034 cm^{-1} and core power fraction is 44%. So, at optimum design parameters, the obtained EML is obviously better than the previously reported [9,25–32,37] optical waveguides.

Core power fraction as a function of frequency at different polarization modes and other optimal design parameters is shown in Fig. 6 where it is observed that as the frequency increases the core power fraction also increases. This is because, with the increase of frequency some of the useful power tends to penetrate throughout the cladding region. It can be seen from Fig. 6 that at 1 THz frequency, x-polarization mode and other optimal design parameters the obtained core power fraction is 44%.

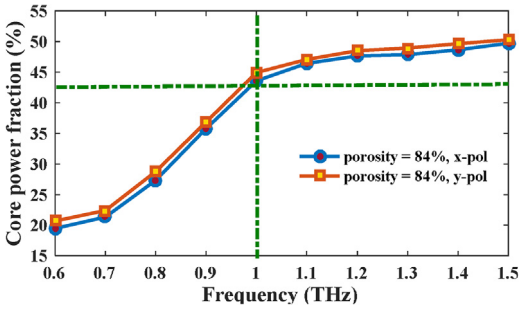

Fig. 6. Core power fraction vs frequency at optimal design parameters for orthogonal polarization modes.

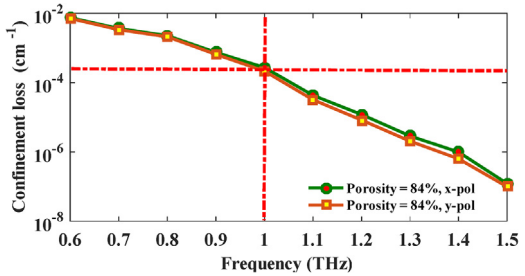

Fig. 7. Confinement loss with respect to frequency at optimal design parameters.

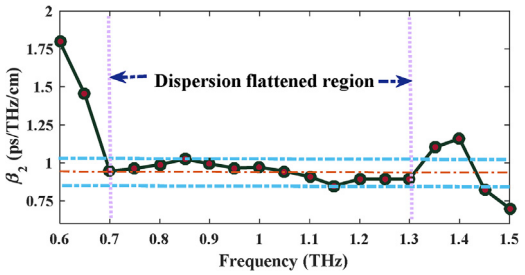

Fig. 8. Dispersion variation vs frequency at optimal design parameters.

Confinement loss is another important guiding property of terahertz PCF. It can limit the length of thereal terahertz transmission system. Confinement loss of the proposed waveguide can be calculated by [41],

$$\alpha_{CL} = \frac{4\pi f}{c}\mathrm{Im}(n_{eff}),\mathrm{cm}^{-1} \tag{3}$$

where, f is the operating frequency, c is the speed of light and $\mathrm{Im}(n_{eff})$ represents the imaginary part of the complex refractive index. Confinement loss actually depends on the core porosity and number of air holes used in the cladding. Fig. 7 shows the characteristics of confinement loss with respect to frequency. Here it is observed that, as the frequency increases, confinement losses are scaled down. This is because, as the frequency increases more light start to constrict strongly in the porous core region. By increasing the number of air holes in the cladding the confinement loss can be reduced further. At optimal design parameters, the obtained confinement loss is in the order of $10^{-3.7}$ cm^{-1} that is improved over previously reported designs [28–32,37].

Dispersion is an important property that must be observed for an efficient waveguide design. In our proposed waveguide, material dispersion is totally neglected, where only waveguide dispersion is measured as Topas has aconstant refractive index over the frequency ranges of 0.1–1.5 THz. Waveguide dispersion can be calculated using the following equation [32],

$$\beta_2 = \frac{2}{c}\frac{dn_{eff}}{d\omega} + \frac{\omega}{c}\frac{d^2n_{eff}}{d\omega^2} \tag{4}$$

where, $\omega = 2\pi f$ is the angular frequency and c is the speed of light in vacuum.

Fig. 8 describes the behavior of dispersion variation with respect to frequency. It is observed that, a flattened dispersion of 0.94 ± 0.09 ps/THz/cm is obtained within a broad frequency range of 0.70–1.3 THz, which is significant for terahertz communication applications. The obtained dispersion is more flat than the previously reported [28,29,31,32]. So, considering

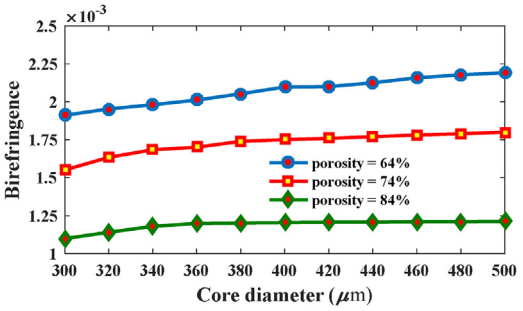

Fig. 9. Birefringence vs core diameter at optimal design parameters.

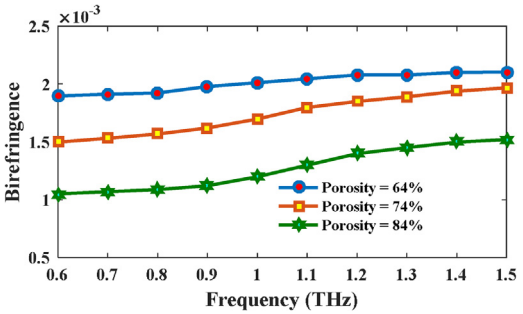

Fig. 10. Birefringence vs frequency at optimal design parameters.

different characteristics like EML, core power fraction, confinement loss and dispersion the fiber operating range is set to 0.7-1.3 THz.

In order to consider a PCF as polarization maintaining terahertz fiber, the index differences between x-polarization and y-polarization mode should be as high as possible. These index differences is called birefringence that can be calculated by [31],

$$B = |n_x - n_y| \tag{5}$$

where, B indicates birefringence, n_x and n_y indicates the refractive indices of *x* and *y* polarizations respectively.

The variation of birefringence with respect to core diameter at different core porosities is shown in Fig. 9. It can be observed that, as the core diameter increases the birefringence also increases as some of the useful power starts to penetrate outside the core that reduces the index contrast between the polarization modes. Fig. 10. indicates the variation of birefringence with respect to frequency at different porosity values. It is observed that, as the porosity increases the amount of birefringence decreases. It is also observed that, birefringence increases with the increase of frequency. The reason is, with the increase of frequency the index contrast between the orthogonal polarization modes increases and hence the phenomenon happened. From Fig. 9 and 10 it can be observed that, at optimal design parameters the value of birefringence is 1.23×10^{-3}.

The modal effective area is a qualitative measurement of the cross section area covered by the guided mode of the fiber. The fundamental mode area can be calculated by [36],

$$A_{eff} = \frac{\left[\int I(r)\,rdr\right]^2}{\left[\int I^2(r)\,dr\right]^2} \tag{6}$$

where, $I(r) = |E_t|^2$ indicates the distribution of electric field intensity across the cross section of the proposed fiber.

Fig. 11 reveals the affect of frequency on the effective mode area. Modal effective area depends largely on the frequency of the guided mode. It is observed that as the frequency increases, the A_{eff} decreases smoothly. The reason being more light is confined in the core for $f > 1$ THz and as the frequency increases light starts to penetrates towards the cladding. The obtained A_{eff} is very much comparable with the previously reported [27,36–38] optical waveguides.

Figure of Merit (FOM) is also an important property of a fiber that is necessary for overall assessment of a PCF. FOM can be calculated as the ratio of the normalized value of effective material loss to the obtained value of modal effective area [26,37],

$$FOM = {}^{\alpha_{eff}}\!/_{A_{eff}} \tag{7}$$

where, α_{eff}indicates the normalized value of EML and A_{eff} symbolizes the obtained value of modal effective area.

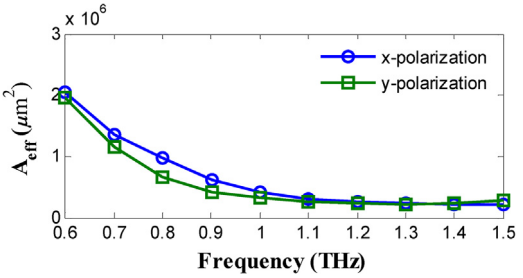

Fig. 11. Modal effective area vs frequency at optimal design parameters.

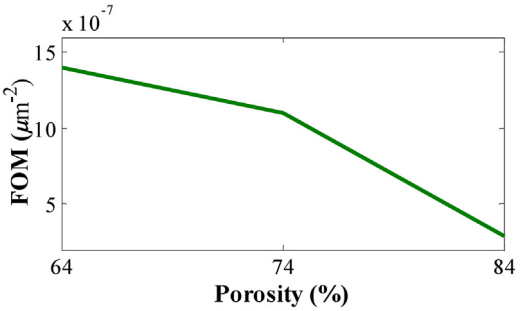

Fig. 12. FOM vs porosity at D_{core} = 360 μm and f = 1 THz.

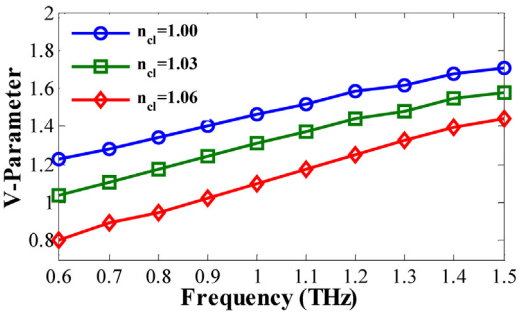

Fig. 13. V-parameter vs frequency at D_{core} = 360 μm and porosity = 84%.

It can be observed from Fig. 12 that FOM decreases with the increase of porosity. The reason is, with the increase of porosity the value of EML decreases significantly (see Fig. 3).So, from Fig. 12 it can be said that there is a significant control of α_{eff} over FOM where A_{eff} has no considerable control over it as the value of A_{eff} is negligible compared to α_{eff}. Lower value of A_{eff} have very useful applications in nonlinear effects of a PCF.

Now, it has to be ensured that the proposed fiber operates in the single mode condition. The single mode characteristics of a fiber can be calculated by the following equation [32],

$$V = \frac{2\pi r f}{c}\sqrt{{n_{co}}^2 - {n_{cl}}^2} \leq 2.405. \tag{8}$$

So, a fiber to be operated in single mode condition, it must satisfy the condition of V–parameter. In Eqn. 8, n_{co} indicates the effective refractive index of the porous core which is equal to (n_{eff}) [37] and n_{cl} indicates the refractive index of cladding. Ideally the value of n_{cl} is considered to be unity [27–32] as major portion of the cladding consists of circular air holes and the refractive index of air is unity. Practically, the value of n_{cl} should not be unity because the cladding not only consists of air but also Topas, so practically the refractive index of the cladding should be slightly greater than unity [38]. In our designed fiber, the V-parameter is calculated for different values of n_{cl} with respect to core diameter and frequency. Figs. 13 and 14 indicate that the value of V does not exceed 2.405 that confirm the single mode operation of the fiber.

Finally, a characteristics comparison of the previously reported waveguides and our proposed waveguide is shown in Table 1.

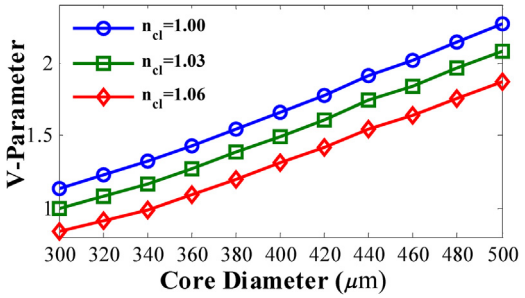

Fig. 14. V parameter vs core diameter at optimal values.

Table 1
Comparison of the proposed fiber with previously reported fiber.

References	Frequency (THz)	Porosity (%)	EML (cm^{-1})	Dispersion Variation (ps/THz/cm)	Confinement loss (cm^{-1})
[27]	1	60%	0.07	–	–
[28]	1	60%	0.066	0.30	$10^{-3.5}$
[29]	1	68%	0.053	0.25	10^{-4}
[30]	1	80%	0.076	0.086	10^{-3}
[31]	1	–	0.089	0.27	$10^{-2.5}$
[32]	1	79%	0.047	0.15	10^{-3}
[37]	1	81%	0.043	0.09	$10^{-3.5}$
[41]	1	70%	0.035	0.13	0.0012
This Manuscript	1	84%	0.034	0.09	$10^{-3.7}$

4. Conclusion

We have presented the numerical modeling of a single mode terahertz PCF with ultra low effective material loss, negligible confinement, higher effective mode area and ultra flattened dispersion properties. At optimal design parameters, the proposed fiber demonstrates a lower EML of 0.034 cm^{-1}, core power fraction of 44%, confinement loss of the order of $10^{-3.7}$ cm^{-1}, birefringence of 1.23×10^{-3}, near zero flattened dispersion of 0.94 ± 0.09 ps/THz/cm over a broad frequency range of 0.70–1.30 THz and higher modal effective area of 0.6×10^6 μm^2. The obtained ultra low loss, high birefringence and dispersion-flattened properties of the fiber potentially have a significant application in longer distance terahertz wave transmission as well as polarization maintaining applications. Again, simplicity in design and the realistic size makes it feasible in terms of fabrication. So, considering all the aforementioned properties, we can conclude that, if the proposed fiber can be utilized properly with state of the art technology then it will open a new window for longer distance transmission of terahertz waves.

References

[1] N. Chen, J. Liang, L. Ren, High-birefringence, low-loss porous fiber for single-mode terahertz-wave guidance, Appl. Opt. 52 (7) (2013) 5297.
[2] D. Abbott, X.C. Zhang, T-ray imaging, sensing, and retection, Proc. IEEE 95 (8) (2007) 1509–1513.
[3] M.M. Awad, R.A. Cheville, Transmission terahertz waveguide based imaging below the diffraction limit, Appl. Phys. Lett. 86 (2005) 221107.
[4] G.M. Png, R.J. Falconer, D. Abbott, Tracking aggregation and fibrillation of globular proteins using terahertz and far-infrared spectroscopies, IEEE Trans. Terahertz Sci. Technol. 6 (1) (2016) 45–53.
[5] D.J. Cook, B.K. Decker, M.G. Allen, Quantitative THz spectroscopy of explosive materials, Proc. of OSA Conf. on Optical Terahertz Science and Technology (2005) (Art. No. MA6).
[6] Y. Sun, Z. Zhu, S. Chen, J. Balakrishnan, D. Abbott, A.T. Ahuja, E. Pickwell-MacPherson, Observing the temperature dependent transition of the gp2 peptide using terahertz spectroscopy, PLoS One 7 (11) (2012) e50306.
[7] K. Kawase, Y. Ogawa, Y. Watanabe, H. Inoue, Non-destructive terahertz imaging of illicit drugs using spectral fingerprints, Opt. Express 11 (2003) 2549–2554.
[8] M. Nagel, P.H. Bolivar, M. Brucherseifer, H. Kurz, A. Bosserhoff, R. Bttner, Integrated THz technology for label-free genetic diagnostics, Appl. Phys. Lett. 80 (2002) 154––156.
[9] M.I. Hasan, S.M.A. Razzak, G.K.M. Hasanuzzaman, M.S. Habib, Ultra-low material loss and dispersion flattened fiber for THz transmission, IEEE Photonic Technol. Lett. 26 (2014) 2372–2375.
[10] S. Atakaramians, V.S. Afshar, T.M. Monro, D. Abbott, Terahertz dielectric waveguides, Adv. Opt. Photonics 5 (2) (2013) 169–215.
[11] R. Mendis, D. Grischkowsky, Plastic ribbon THz waveguides, J. Appl. Phys. 88 (2000) 4449–4451.
[12] K. Wang, D.M. Mittleman, Metal wires for terahertz wave guiding, Nature 432 (2004) 376–379.
[13] H. Bao, K. Nielsen, O. Bang, P.U. Jepsen, Dielectric tube waveguides with absorptive cladding for broadband, low-dispersion and low loss THz guiding, Sci. Rep. 5 (2015) 1–9.
[14] M. Goto, A. Quema, H. Takahashi, S. Ono, N. Sarukura, Teflon photonic crystal fiber as terahertz waveguide, Jpn. J. Appl. Phys. Part 2 43 (2004) 317–319.
[15] C.S. Ponseca, R. Pobre, E. Estacio, N. Sarukura, A. Argyros, M.C. Large, M.A. van Eijkelenborg, Transmission of terahertz radiation using a microstructured polymer optical fiber, Opt. Lett. 33 (2008) 902–904.

[16] H. Han, H. Park, M. Cho, J. Kim, Terahertz pulse propagation in a plastic photonic crystal fiber, Appl. Phys. Lett. 80 (2002) 2634–2636.
[17] G. Emiliyanov, J.B. Jensen, O. Bang, P.E. Hoiby, L.H. Pedersen, E. Kjaer, L. Lindvold, Localized bio-sensing with Topasmicro-structured polymer optical fiber, Opt. Lett. 32 (2007) 460–462.
[18] X. Tang, Y. Jiang, B. Sun, J. Chen, X. Zhu, P. Zhou, D. Wu, Y. Shi, Elliptical hollow fiber with inner silver coating for linearly polarized terahertz transmission, IEEE Photon. Technol. Lett. 25 (2013) 331–334.
[19] C. Markos, A. Stefani, K. Nielsen, H.K. Rasmussen, W. Yuan, O. Bang, High-Tg TOPAS microstructured polymer optical fiber for fiber Bragg grating strain sensing at 110 degrees, Opt. Express 21 (4) (2013) 4758–4765.
[20] G. Emiliyanov, J.B. Jensen, O. Bang, P.E. Hoiby, L.H. Pedersen, E.M. Kjaer, L. Lindvold, Localized bio-sensing with TOPAS micro-structured polymer optical fiber, Opt. Lett. 32 (5) (2007) 460–462.
[21] W. Yuan, L. Khan, D.J. Webb, K. Kalli, H.K. Rasmussen, A. Stefani, O. Bang, Humidity insensitive TOPAS polymer fiber Bragg grating sensor, Opt. Express 19 (20) (2011) 19731–19739.
[22] K. Nielsen, H.K. Rasmussen, A.J.L. Adam, P.C.M. Planken, O. Bang, P.U. Jepsen, Bendable, low-loss TOPAS fibers for the terahertz frequency range, Opt. Express 17 (10) (2009) 8592–8601.
[23] J. Balakrishnan, B.M. Fischer, D. Abbott, Sensing the hygroscopicity of polymer and copolymer materials using terahertz time-domain spectroscopy, Appl. Opt. 48 (12) (2009) 2262–2266.
[24] G. Woyessa, A. Fasano, A. Stefani, C. Markos, K. Nielsen, H.K. Rasmussen, O. Bang, Single mode step-index polymer optical fiber for humidity insensitive high temperature fiber Bragg grating sensors, Opt. Express 24 (2016) 1253–1260.
[25] H.L. Bao, K. Nielsen, H.K. Rasmussen, P.U. Jepsen, O. Bang, Fabrication and characterization of porous-core honeycomb bandgap THz fibers, Opt. Express 20 (2012) 29507–229517.
[26] J. Liang, L. Ren, N. Chen, C. Zhou, Broadband, low-loss, dispersion flattened porous core photonic band gap fiber for terahertz (THz) wave propagation, Opt. Commun. 295 (2013) 257–261.
[27] S.F. Kaijage, Z. Ouyang, X. Jin, Porous-core photonic crystal fiber for low loss terahertz wave guiding, IEEE Photonics Technol. Lett. 25 (15) (2013) 1454–1457.
[28] R. Islam, G.K.M. Hasanuzzaman, M.S. Habib, S. Rana, M.A.G. Khan, Low-loss rotated porous core hexagonal single-mode fiber in THz regime, Opt. Fiber Technol. 24 (2015) 38–43.
[29] M.S. Islam, S. Rana, H. Rahman, J. Sultana, Porous core photonic crystal fiber for ultra-low material loss in THz regime, IET Commun. 10 (16) (2016) 2179–2183.
[30] M.R. Hasan, M.A. Islam, R. Ahmmed, A single mode porous-core square lattice photonic crystal fiber for THz wave propagation, J. Eur. Opt. Soc.-Rapid Publ. 12 (2016) 1, http://dx.doi.org/10.1186/s41476-016-0017-5.
[31] M.I. Hasan, M.S. Habib, M.S. Habib, Design of hybrid photonic crystal fiber: polarization and dispersion properties, Photonics Nanostruct. Fundam. Appl. 12 (2) (2014) 205–211.
[32] M.S. Islam, M.R. Islam, M. Faisal, A.S.M. ShamsulArefin, H. Rahman, J. Sultana, Extremely low loss, dispersion-flattened porous core photonic crystal fiber for THz regime, Opt. Eng. 55 (7) (2016) 076117.
[33] Fabrications of photonic crystal fibers, Photonic crystal fiber, science[online]available:http://www.mpl.mpg.de/en/russell/research/topics/fabrication.html. [Accessed: 31st March 2017].
[34] K.M. Kiang, K. Frampton, T.M. Monro, R. Moore, J. Tucknott, D.W. Hewak, D.J. Richardson, H.N. Rutt, Extruded single-mode non-silica glass holey optical fibres, Electron. Lett. 38 (12) (2002) 546–547.
[35] R.T. Bisen, D.J. Trevor, Solgel-derived micro-structured fibers: fabrication and characterization, Optical Fiber Communication Conference (2005), http://dx.doi.org/10.1109/OFC.2005.192772 (Technical Digest. OFC/NFOEC).
[36] J.J. Bai, J.N. Li, H. Zhang, H. Fangand, S.J. Chang, A porous terahertz fiber with randomly distributed air holes, Appl. Phys. B 103 (2) (2011) 381–386.
[37] M.S. Islam, Sultana Rana, S. Islam, M.R. Faisal, M. Kaijage, S.F. Abbott, Extremely low material loss and dispersion flattened TOPAS based circular porous fiber for long distance terahertz wave transmission, Opt. Fiber Technol. 24 (2016) 6–11.
[38] M.S. Islam, J. Sultana, J. Atai, D. Abbott, S. Rana, M.R. Islam, Ultra low loss hybrid core porous fiber for broadband applications, Appl. Opt. 56 (9) (2017) 1232–1237.
[39] M. Uthman, B.M.A. Rahman, N. Kejalakshmy, A. Agrawal, K.T.V. Grattan, Design and characterization of low-loss porous-core photonic crystal fibre, IEEE Photonics J. 4 (6) (2012) 2315–2325.
[40] A. Aming, M. Uthman, R. Chitaree, W. Mohammed, B.M.A. Rahman, Design and characterization of porous core polarization maintaining photonic crystal fiber (PCF) for THz guidance, IEEE/OSA J. Lightwave Technol. 34 (23) (2016) 5583–5590.
[41] G.K.M. Hasanuzzaman, M.S. Habib, S.M.A. Razzak, M.A. Hossain, Y. Namihira, Low loss single-mode porous-core kagome photonic crystal fiber for THz wave guidance, J. Lightwave Technol. 33 (2015) 4027–44031.